

# High Performance Thermal Straps for a Full Range of Application Temperatures

M. Ralphs, M. Sinfield, M. Felt

Space Dynamics Laboratory  
North Logan, UT 84341

## ABSTRACT

Thermal straps are an essential component when using vibration sensitive instruments and cryocoolers in close proximity. Thermal straps conduct heat from the instrument to the cryocooler while limiting the amount of mechanical vibration the cryocooler transfers back to the instrument. Thermal straps are made from flexible, thermally conductive materials. Traditionally, they are made of metal – aluminum or copper, mostly – that has been formed into thin foils, wires, or braids to provide greater flexibility while still providing good thermal conductivity. These metallic straps, if made from pure metals, provide superior thermal performance at cryogenic temperatures ( $< 60$  K) where their thermal conductivities peak to extraordinary levels. Pyrolytic graphite sheet (PGS) thermal straps have a thermal conductance that peaks at higher temperatures – approximately 160 K – and provide much higher mass-specific thermal conductance at temperatures above 60 K than metallic straps. This paper discusses the pros and cons of aluminum, copper, and PGS thermal straps along with different techniques to test their thermal and mechanical performance.

## INTRODUCTION

Thermal straps conduct heat while minimizing mechanical strain and vibration between system components.[1–4] They are often used with cryocoolers to transfer waste heat to be rejected because they can thermally couple a system to the cryocooler, while still offering some level of mechanical isolation.[5] This mechanical isolation while maintaining thermal transport is critical in a spacecraft with a focal plane array that is sensitive to mechanical vibration.[4] Thermal straps are also used in systems where coefficient of thermal expansion (CTE) mismatches would create a mechanically over-constrained system and create high stresses in the system or where component movement is required between two adjacent components that need to have a thermal connection to each other. Simply put, thermal straps transfer heat, provide some level of mechanical flexibility, and are critical in many space and ground applications.

Historically, thermal straps have been made from thin sheets of metal or wires with high thermal conductivity so that they can bend and flex as needed but still provide sufficient thermal transport. For example, Figure 1a shows a thermal strap made from high purity copper wires that are braided into a cable or rope. Metallic foil or braid thermal straps are especially useful at cryogenic temperatures, where their thermal conductivities are elevated above what is typically seen near room temperature. As illustrated in Figure 1b, the thermal conductivity of some high purity metals peak in the range of 10-30K and can reach thermal conductivities that are multiple orders of magnitude

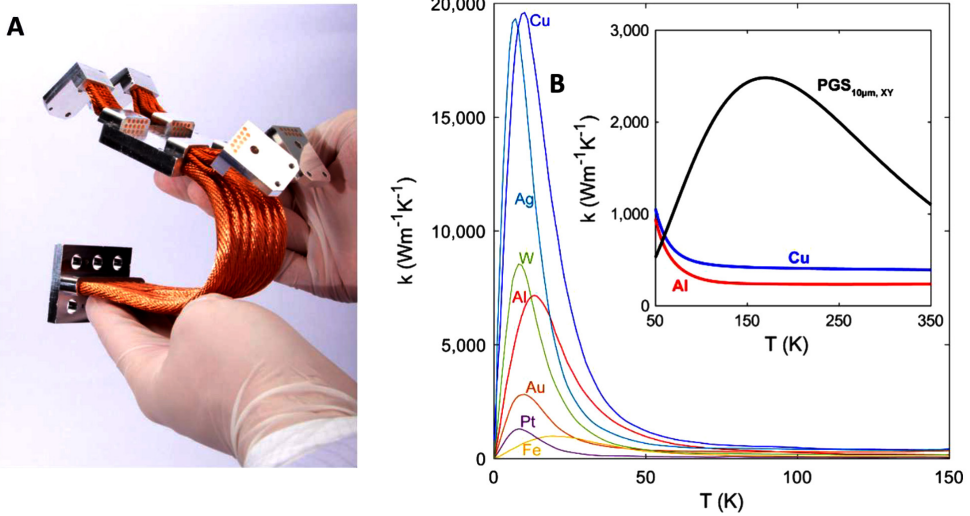


**Figure 1.** (A) Image of a copper braid thermal strap, fabricated by SDL, with several mounting interfaces; (B) a plot of thermal conductivity versus temperature for a variety of common metals;6 and (C) a plot of published thermal conductivity of pyrolytic graphite sheet (PGS) versus temperature [7] as compared to copper and aluminum at warmer temperatures.

above what can be achieved at higher temperatures.[6] Copper and aluminum are the most common materials for metallic thermal straps, with high thermal conductivities and stable mechanical properties, and are commonly seen in wire braid and thin foil thermal straps.

Pyrolytic graphite (PG), in several different forms, is somewhat new to the game of thermal straps but is especially useful at non-cryogenic temperatures. The extraordinary properties of pyrolytic graphite have been known since the early 1900's,[7] but hasn't been used in thermal straps until recently. Annealed pyrolytic graphite (APG) and pyrolytic graphite sheets (PGS) are common forms of PG used in thermal straps in recent years. APG has a very high thermal conductivity but is brittle and is commonly used as a composite within a more structurally sound matrix material. PGS is a more flexible than APG and enables the PG to be used in thermal straps without a matrix material supplying the necessary structural support. PGS has a much higher thermal conductivity than metals at non-cryogenic temperatures with the thermal conductivity curve peaking at over  $2000 \text{ Wm}^{-1}\text{K}^{-1}$ . Figure 1c inset shows the in-plane thermal conductivity of PGS that is  $10\mu\text{m}$  thick. [8] The in-plane conductivity is much higher than the through-plane conductivity, usually by at least an order of magnitude. Thermal strap performance is most often dominated by the in-plane thermal conductivity as they transfer heat between one end block to the other, but shorter straps are affected more than longer straps by the lower through-plane thermal conductivity. The high thermal conductivity that peaks around 160 K, combined with the low density ( $\sim 1.95 \text{ g/cc}$ ) makes PGS ideal for warmer space applications where metallic straps fail to provide sufficient mass-specific thermal performance.

PGS has a range in thermal conductivity, depending on how it is processed, but generally has a higher in-plane thermal conductivity the thinner the sheet is made. From an undisclosed suppliers' datasheet (trade secret), PGS that is  $100\mu\text{m}$  thick has  $k_{xy} = 700 \text{ Wm}^{-1}\text{K}^{-1}$  while PGS that is  $17\mu\text{m}$  thick has  $k_{xy} = 1750 \text{ Wm}^{-1}\text{K}^{-1}$  at room temperature. The through-plane conductivity scales inversely to this trend, with  $k_z = 26 \text{ Wm}^{-1}\text{K}^{-1}$  at  $100\mu\text{m}$  and only  $11 \text{ Wm}^{-1}\text{K}^{-1}$  at  $17\mu\text{m}$ . This trend is illustrated in Figure 2b with the change in density as the thickness scales illustrated in Figure 2a.

Similar to how the thermal conductivity of PGS depends on how it's processed, metallic foil and braids are dependent on how they are processed. There are many factors that contribute to the thermal conductivity of metallic foils and braids used in thermal straps (alloy, defects, work hardening, etc.), but, ultimately, the purer the metal the higher the thermal conductivity. This is because the higher the

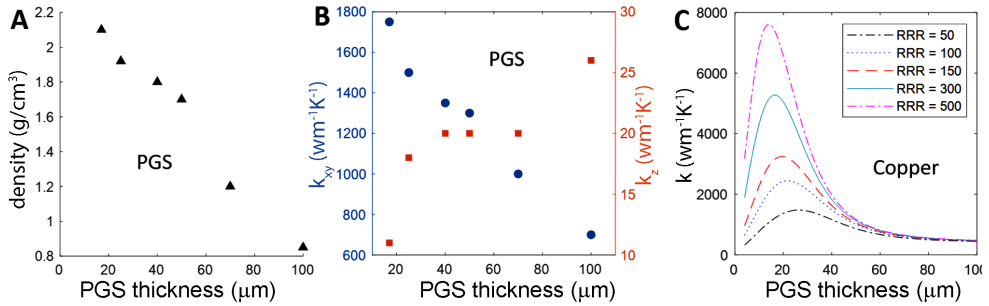


**Figure 2.** PGS properties from an undisclosed suppliers' data sheet for (A) density and (B) thermal conductivity. (C) Thermal conductivity of Copper OFHC versus temperature at various levels of RRR from NIST. [9]

purity of the metal, in general, the fewer defects and the longer the mean free path.[10] One metric that is used to gauge the thermal conductivity of the metal is the residual resistivity ratio (RRR). The RRR of a material is the ratio of the electrical resistivity of the material at room temperature and at 0K, or an estimate of what it would be at 0K.[11] Since the thermal conductivity of a metal is dominated by electron thermal transport, this RRR measurement of electrical resistivity directly applies to the measure of thermal conductivity. The relationship between electrical conductivity and thermal conductivity for metals as a function of temperature is known as the Wiedemann-Franz law.[12] Figure 2c demonstrates how the thermal conductivity of copper depends on the RRR of the copper, especially at cryogenic temperatures. Copper that SDL procures usually has a RRR of 150-350, corresponding to a peak thermal conductivity of 3000-5500 Wm<sup>-1</sup>K<sup>-1</sup>.

SDL has been researching and fabricating thermal straps for more than 2 decades and has built and tested thermal straps for many space missions over the years, including James Webb Space Telescope (JWST), Mars Curiosity rover, and Ionospheric Connection Explorer (ICON) MIGHTI, to name only a few. SDL has a dedicated branch for thermal straps and thermal technologies and is ISO 9001 certified.

This paper will demonstrate how the many varieties of thermal straps produced by SDL provide high thermal performance and flexibility for application temperatures ranging from cryogenic to beyond room temperature. Furthermore, results from various thermal and mechanical tests will present the pros and cons of various strap types and materials.

## METHODS

### Thermal Conductance Testing

Thermal conductance measurements are critical in measuring the performance of a thermal strap. Thermal conductance tests at SDL are done in thermal vacuum chambers built specifically to test the thermal conductance of thermal straps. Several of these chambers use cryocoolers and can test the performance between 25K and 323K. One chamber is capable of using a liquid bath as the cold sink and is thus capable of utilizing liquid helium in order to test down to 4K. Straps are bolted to the temperature controlled cold plate, covered in MLI, a cold shroud is bolted to the same cold plate, and the cold shroud is again blanketed in MLI. Wires are thermally grounded to the cold plate with enough slack to prevent a significant thermal short to the hot end of the strap. These are all precautions taken to minimize thermal parasitic loads and sources for the conductance test.

Silicon diodes are predominantly used in thermal conductance tests and are either bolted or bonded to the straps and fixtures. Various heaters are used to provide heat to the hot end of strap to produce the desired temperature gradient. Strap conductance,  $G$ , can be measured with the input heat,  $Q$ , and the measured temperature gradient across the strap,  $\Delta T$ , by

$$G = Q / \Delta T. \quad (1)$$

However, the uncertainty in using this calculation is subject to the bias uncertainty of power and the temperature sensors. This method is still applied in some special occasions at SDL, but most conductance measurements use three power levels input to the hot end of the strap and look at the slope of the line fit of  $Q$  vs  $\Delta T$ . This helps eliminate some of the correlated bias uncertainties in the measurement and minimizes the need for calibrated temperature sensors. The standard error associated with the linear regression - also known as the coefficient of variation (CoV) - can then be used to estimate the uncertainty in the measurement, as suggested in chapter 8 of Coleman and Steele.[13] The instrumentation uncertainty, estimated by a Taylor Series Method (TSM) uncertainty analysis is generally much smaller than the standard error of the linear regression.

Variation in conductance test results is generally small, especially when sensor placement is repeatable. Test-to-test variation is measured when the test is taken down and re-setup, including bonding or installing sensors back onto the strap and installing it back into the conductance chamber. Test-to-test variation, as measured over a 2-year period and multiple strap designs, has been calculated to have a standard deviation of 4.12%. This means that if a particular thermal strap is re-tested under that same parameters as a previous test but the test is re-setup from scratch, that the measured conductance is expected to be within 4.12% of the previous measurement, 68% of the time. This variation is mainly due to the repeatability of sensor placement, but other factors – such as placement in the conductance chamber, dwell time at temperature, parasitic heat loads, and fastener torque values - can also contribute. Short term repeatability is when the strap setup has not changed and the strap has not been taken out of the chamber, but the temperature may have been cycled or the test repeated over multiple days. Short term test repeatability generally only includes random variation – such as chamber temperature drift and readout error – and has been measured to have a standard deviation of 0.57% of the measured conductance.

### **Thermal Cycle Testing**

Thermal straps, especially those designed to go into space, are commonly subjected to various interludes at different temperatures. Thermal straps can be built with more than one material and the various coefficients of thermal expansion can cause thermal stresses. Thermal cycle testing involves cycling the test article between the expected hot and cold temperatures to ensure that thermal stresses do not cause degradations in performance or failures. Conductance tests before and after the thermal cycling provide insight into whether any degradation occurred from the thermal stresses in the straps. Thermal cycle testing is usually done in a vacuum chamber.

### **Flexibility or Stiffness Testing**

Strap flexibility, or stiffness, is often important to determine the mechanical impact the strap will have on interfacing components. The stiffness is measured by holding one end of the strap stationary, moving the other end, and measuring the force required to do so.

### **Fatigue Testing**

Fatigue testing involves moving one end of a strap with respect to the other end then repeating that movement many times. This test is important in some strap designs where the normal operation of the strap may involve displacements and the longevity and life of the strap must be verified. This testing can either be carried out with finite displacements and finite number of cycles or by using specific fixturing and a shaker table to exercise the thermal strap in a way that fatigues the necessary components.

### **Thermal Modelling and Analysis**

With many thermal strap designs, a standard thermal resistance model can provide a decent estimate on thermal performance.[14] However, for a more accurate estimate of a strap's thermal performance, a finite element model is made that uses correlated values from historic, similar strap designs. See SDL's presentation on thermal modelling of thermal straps at Spacecraft Thermal Control Workshop 2018 for more details.[15]

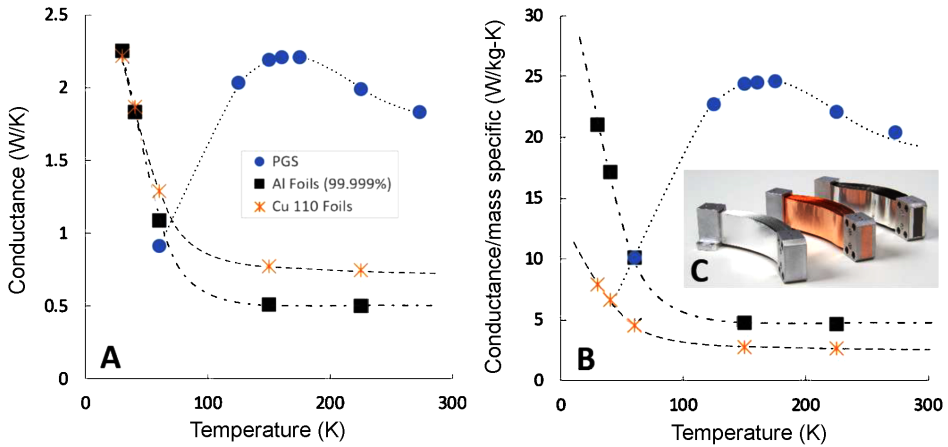


**Figure 3.** Thermal conductance (A), mass-specific thermal conductance (B), and a photo (C) of straps A, B, and C (PGS, Copper OFE, 99.999% Al).

## RESULTS AND DISCUSSION

### Thermal Strap Conductance

The thermal performance of thermal straps is highly dependent on the strap geometry. For this reason, a single strap geometry was fabricated, but with three different materials for the flexible portion. Aluminum 1100-H112 was used for the end blocks which were swaged onto the flexible portions. The three flexible materials were 0.001” thick: PGS, 0.001” thick OFE copper, and 0.001” thick 99.999% pure aluminum and will be referred to in this work as straps “A”, “B”, and “C”, respectively. These three straps, shown in Figure 3c, were conductance tested over a range of temperatures to compare and contrast thermal performance over a broad spectrum of temperatures.

As is evident in Figure 3a, the copper and aluminum foil straps perform best at cryogenic temperatures where their thermal conductivity spikes and the PGS performs best above 70K. The mass-specific conductance, shown in Figure 3b, shows much better performance in the aluminum straps at cryogenic temperatures since it’s density is 30% that of copper (2.7 g/cc for al and 8.96 g/cc for copper) and the PGS performs even better at warmer temperature with a density ~73% that of aluminum (1.95 g/cc for 25 $\mu$ m PGS). While actual performance will vary depending on the geometry of the strap, these temperature dependent trends apply to all straps that use these materials.

### Thermal Cycling and PGS Recession

Metallic strap thermal performance historically is not affected by thermal cycling. PGS thermal straps, however, can show slight degradations in the thermal performance due to what is currently suspected as PGS recession from thermal cycling where the PGS dead ends in the straps’ interfacing surface. This phenomenon and its current investigation is limited to PGS straps with aluminum end blocks. The CTE mismatch between these two materials as the straps undergo thermal cycling to temperatures below the target test temperature cause the PGS to recede from the interfacing surface. This recession causes a decrease in the interface area between the strap and interfacing hardware, as illustrated in Figure 4, which can lead to a degradation in thermal performance. The CTE mismatches and associated thermal stresses can cause greater failures in straps that are assembled with adhesives or solders, but SDL’s proprietary assembly process uniquely minimizes the negative impacts of this phenomenon to a slight decrease in thermal performance (3-7% loss of total strap conductance).

Measurements taken with a calibrated coordinate measurement machine (CMM) and profilometer indicate the PGS recedes from the interface 0.001-0.002 inches in normal circumstances. A

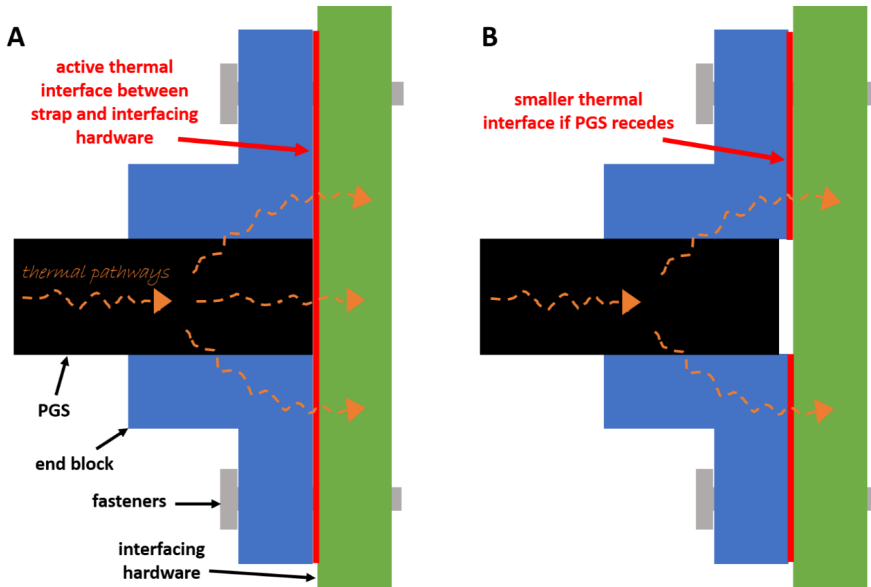


**Figure 4.** Illustration of (A) the full thermal interface between a thermal strap and mating hardware and (B) how PGS recession can cause degraded thermal performance if the PGS dead-ends in the strap to mating hardware interface by decreasing the interfacing area.

PGS thermal strap was repeatedly submerged and allowed to stabilize in liquid nitrogen (LN2) and then brought back to room temperature to exacerbate this issue. This strap showed PGS recession of up to 0.003 inches in some locations. The PGS recession on this strap was measured after each submersion in LN2 and ~90% of the recession took place after the first submersion in LN2, suggesting the strap stabilizes quickly and does not continue to degrade.

Thermal cycling has been done on several strap designs where the PGS dead ends in the strap interface to quantify and characterize the effect of PGS recession on thermal strap conductance. PGS straps J and K will be used to illustrate the phenomenon in this work. The straps were thermal cycled between 120K and 313K between each conductance test. Conductance tests were performed with a thermal strap average temperature of 235K. Figure 5 inset shows a photograph of one of the straps. The other strap was slightly longer but similar in geometry. Figure 5 demonstrates that most of the performance degradation occurs from the first thermal cycle and the total amount of degradation ranges from 3-7% of the original strap conductance. This range has held true for all the PGS straps tested to date that have a geometry where both ends of the PGS are part of the interfacing surface.

### Vibration Testing and Isolation

Thermal straps are often tested as to their ability to survive vibration launch loads and, because of the unique and proprietary swaging process used at SDL, rarely have issues surviving these launch loads. Historical thermal strap vibrate tests have been able to impart up to 68 grms to the straps and produce relative end-to-end displacements of more than  $\pm 1$  inch, independently. One additional measurement that is critical in a thermal strap but is measured less often, is its ability to isolate components from vibration.

A plethora of thermal straps of many types and geometries have been subjected to vibration test loads over the last two decades at SDL. Many straps have been tested to 2-4 orders of magnitude beyond the load and displacements they would see during planned operation and still survived without issue. To demonstrate representative behavior of a thermal strap and how it isolates components from vibration, a short PGS thermal strap has been chosen for this work. Figure 6a shows a PGS thermal strap that will be known as strap “D” in this work. SDL’s patent pending exterior protective

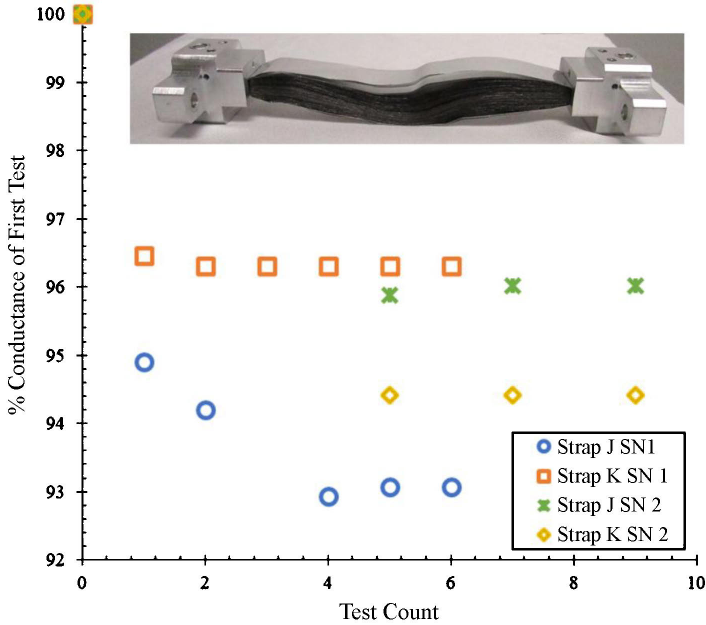


**Figure 5.** PGS strap conductance decrease as a percentage from the original strap conductance with thermal cycling in between each test for straps J and K.

aluminum foils<sup>16</sup> are visible in this photo. Figure 6b shows this strap with a particle containment sleeve (PCS) installed on the strap and the strap installed on the vibration table shaker head with one end of the strap attached to a stationary arm. Control accelerometers are installed on the fixture attached to the vibrate head and a tri-axis accelerometer is attached to the stationary fixture. Figure 7 shows the random control inputs of the vibrate test as well as the resulting forces on the stationary end of the strap. This small, compact PGS strap decreased the input load of 47.8 grms down to 1 grms on the stationary side of the strap.

**Radiation testing**

Some space mission payloads are subjected to high levels of radiation. Heat pipes, commonly used in the same capacity as thermal straps, can degrade from high doses of radiation which may

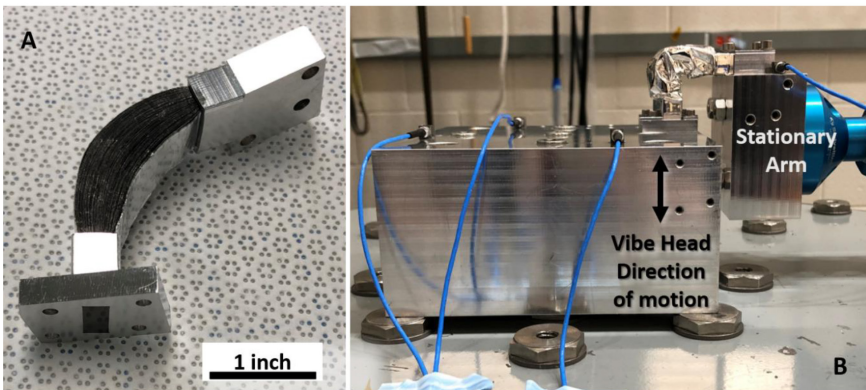


**Figure 6.** PGS thermal strap D (A) without the particle containment sleeve (PCS) and (B) with the PCS and installed on the vibrate table.

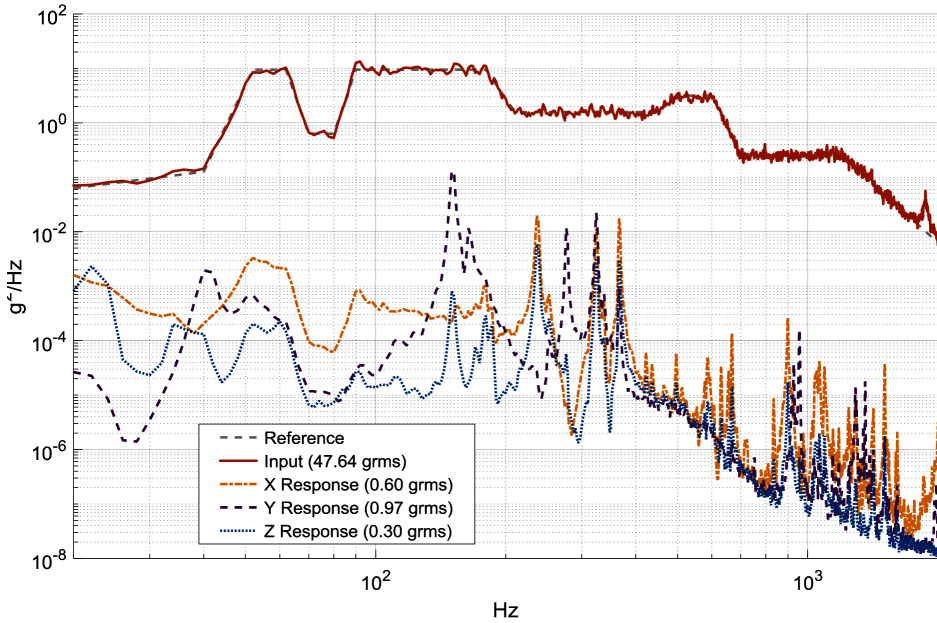


**Figure 7.** Vibration loads applied to PGS thermal strap “ABC” along with the load measured on the static end of the strap.

lead to degraded thermal performance and mission failure. PGS straps, however, were tested and have been shown to be stable after being exposed to high levels of radiation and still provide the required thermal conductance. PGS thermal strap A was subjected to 40 Mrad’s of radiation at a dose of 215.17 rad/sec (to simulate the radiation expected on Europa Clipper) and showed no degradation in thermal conductance, as observed from pre- and post-thermal conductance testing. Furthermore, the mechanical properties of the strap were unchanged, as evaluated from stiffness testing before and after exposure to radiation. Additional radiation exposure to high energy protons and subsequent testing is underway.

**Stiffness Testing**

The stiffness or flexibility of a strap is highly dependent on the strap geometry; however, certain trends are present. Copper braid thermal straps provide the most flexibility in all 3 axes. Copper foil and aluminum foil provide roughly the same magnitude of flexibility. PGS straps are more flexible than aluminum foil straps, as illustrated by Figure 8 with the measured stiffness values for straps A and C, by almost an order of magnitude.

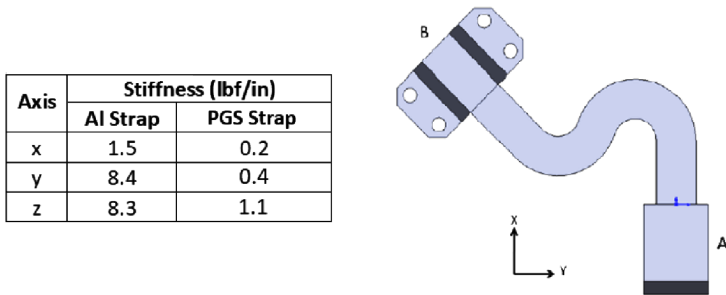


**Figure 8.** Table of measured stiffness values and illustration of measured strap geometry.



### Fatigue testing

Many designs have been fatigue tested over the years at SDL. Some copper foil straps have been tested to 295,000 discrete cycles. Some PGS straps have been tested to discrete 10,000 cycles. Various strap types and designs have been fatigue tested on the shaker table with estimates of the number of cycles well into the hundreds of thousands. No deliverable SDL thermal straps to date have failed from fatigue testing.

### Cleanliness

SDL thermal straps are precision cleaned and their cleanliness certified by SDL's contamination control group (most commonly to IEST-STD-1246). SDL's contamination control group's primary function is to work with delicate optical instruments and sensors and their expertise is leveraged for cleaning and certification on thermal straps. Without a particle containment sleeve (PCS), PGS thermal straps are usually able to be certified to level 300 R5E-1 or better. If particulates of any size or amount are of concern, a PCS can be designed to meet specific requirements; this applies to both PGS and metallic straps. Metallic thermal straps are commonly certified to level 250 R2E-1 or better. Outgassing of SDL PGS straps per ASTM E595 has been measured at 0.01% total mass loss, 0.002% CVC, and 0.008% water vapor regained.

### PGS Embedded Conductor Bar and Radiator

The same proprietary technology for assembling end blocks to PGS is used to embed PGS in conductor bars and radiators. This significantly improves the performance and the ability of these components to spread heat. Figure 9a shows a photo of an aluminum conductor bar with PGS embedded down the entire length of the bar. This prototype performed 4x better than its full aluminum twin. It is common practice to connect a thermal strap to a conductor bar, so integrating the two together to eliminate the interface between them can further improve thermal performance of the system. Figure 9b and 9c depict this concept with the PGS running the entire length of the component – from one interface, through the conductor bar, over the exposed length, and through the end block to the second interface. Furthermore, Figure 9d shows how PGS can be embedded in an aluminum radiator to increase the heat spreading capability and, thus, the thermal efficiency of the radiator. As seen in Figure 9e and Figure 9f, the temperature gradient in the PGS embedded radiator is much smaller than the temperature gradient in the aluminum control unit with the same amount of heat applied. This decrease in gradient represents an increased radiator efficiency.

## CONCLUSIONS

Thermal straps come in all shapes and sizes and can be optimized for maximum thermal performance over a large range of temperatures. Strap material is dependent on application temperature

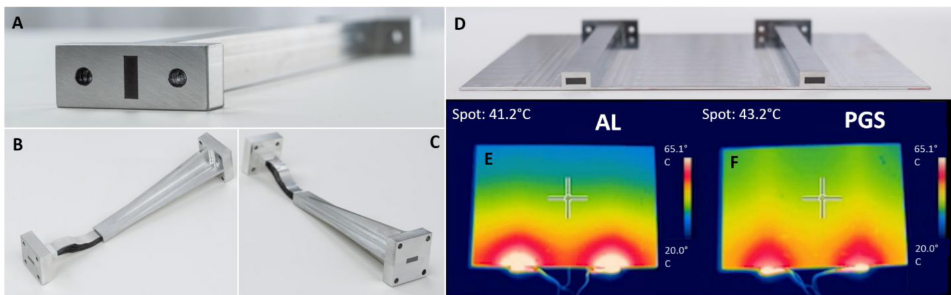


**Figure 9.** (A) PGS embedded aluminum 1100 conductor bar and (B, C) PGS thermal strap in integrated PGS embedded aluminum conductor bar.

and desired mechanical properties with metallic straps providing better thermal performance at cryogenic temperatures (<60K) and PGS straps providing superior performance at warmer temperatures. SDL's heritage, proprietary assembly process provides superior thermal and mechanical properties.

## REFERENCES

1. Bugby, D. & Marland, B. Flexible Conductive Links. in *Spacecraft Thermal Control Handbook, Volume II: Cryogenics* (ed. Donabedian, M.) pp. 327–46 (The Aerospace Press, 2003).
2. Gilmore, D. G. *Spacecraft Thermal Control Handbook. Volume I: Fundamental Technologies*. (The Aerospace Press, 2002).
3. Johnson, D. L. & Ross, R. G. Cryocooler Coldfinger Heat Interceptor. *Cryocoolers 8* 709–717 (1995). doi:10.1007/978-1-4757-9888-3\_70
4. Sparr, L. *et al.* Design and Test of Potential Cryocooler Cold Finger Interfaces. *Adv. Cryog. Eng.* **39**, 1253–62 (1994).
5. Kobayashi, K. & Folkman, S. Stiffness of and Vibration Transmission Through Foil Thermal Links. *Am. Inst. Aeronaut. Astronaut.* **2**, 1495–98 (1998).
6. Powell, R. W., Ho, C. Y. & Liley, P. E. *Thermal Conductivity of Selected Materials. National Standard Reference Data Series - National Bureau of Standards - 8* (1966).
7. Pappis, J. & Blum, S. L. Properties of Pyrolytic Graphite. *J. Am. Ceram. Soc.* (1901).
8. Nakamura, S., Miyafuji, D., Fujii, T., Matsui, T. & Fukuyama, H. Low temperature transport properties of pyrolytic graphite sheet. *Cryogenics (Guildf)*. **86**, 118–122 (2017).
9. Drexler, E. S., Simon, N. J. & Reed, R. P. Properties of copper and copper alloys at cryogenic temperatures. Final report. United States (1992).
10. Sondheimer, E. H. The mean free path of electrons in metals. *Adv. Phys.* **50**, 499–537 (2001).
11. Yin, C. H., Gan, Z. H., Wang, S. H., Liu, D. L. & Qiu, L. M. The Measurement of RRR and Resistance for Aluminum Alloy Based on a Cryocooler. *Cryocoolers 19*, ICC Press, Boulder, CO (2017), pp. 605–612.
12. Chester, G. V. & Thellung, A. The Law of Wiedemann and Franz. *Proc. Phys. Soc.* **77**, 1005–1013 (1961).
13. Coleman, H. W. & Steele, W. G. *Experimentation, Validation, and Uncertainty Analysis for Engineers. AIChE Symposium Series 78*, (Wiley, 2018).
14. Cengel, Y. A. & Ghajar, A. J. *Heat and Mass Transfer: Fundamentals and Applications*. (2016).
15. Felt, M., Sinfield, M., Munns, M., Lloyd, K. & Glaister, D. SDL Flexible Thermal Strap Conductance Measurement, Thermal Model Correlation, and Interface Conductance Variation with Temperature. in *Spacecraft Thermal Control Workshop* (2018).
16. Sinfield, M. & Felt, M. Composite Thermal Strap. U.S. Patent No. 20200307158 (2020).